Optical interrogation of neural circuits in *Caenorhabditis elegans*

Zengcai V Guo[1–3], Anne C Hart[4] & Sharad Ramanathan[1–3]

The nematode *Caenorhabditis elegans* has a compact nervous system with only 302 neurons. Whereas most of the synaptic connections between these neurons have been identified by electron microscopy serial reconstructions, functional connections have been inferred between only a few neurons through combinations of electrophysiology, cell ablation, *in vivo* calcium imaging and genetic analysis. To map functional connections between neurons, we combined *in vivo* optical stimulation with simultaneous calcium imaging. We analyzed the connections from the ASH sensory neurons and RIM interneurons to the command interneurons AVA and AVD. Stimulation of ASH or RIM neurons using channelrhodopsin-2 (ChR2) resulted in activation of AVA neurons, evoking an avoidance behavior. Our results demonstrate that we can excite specific neurons expressing ChR2 while simultaneously monitoring G-CaMP fluorescence in several other neurons, making it possible to rapidly decipher functional connections in *C. elegans* neural circuits.

Understanding the cellular basis of behavior is one of the fundamental challenges in neuroscience. The nematode *Caenorhabditis elegans,* with just 302 neurons, roughly 7,000 synapses, tractable molecular genetic tools and a short generation time provides a unique model system in which to achieve this goal[1]. The physical connectivity and structure of most neurons in *C. elegans* have been determined by serial electron micrography, which delineated most of the chemical synapses and gap junctions in the nervous system[2]. However, this physical information does not address the signal processing capabilities of the corresponding neural circuits; functional information about the connections between neurons is also required. Unfortunately, the dynamics of signaling through *C. elegans* neural circuits and, in most cases, if specific synapses are excitatory or inhibitory, is largely unknown.

Various techniques, including laser microsurgery[3,4] and genetic manipulation[5], have been used to infer neuronal functions. Despite the thick cuticle and the small size of *C. elegans* neurons, electrophysiological techniques have been occasionally used to study neuronal connections *in vivo*[6]. However, electrical recordings can be obtained from only one neuron at a time. Genetically encoded calcium sensors such as G-CaMP[7] and Cameleon[8] have also been used to monitor neural activity[9,10], and there have been notable advances in the use of light-gated cation and chloride channels (channelrhodopsin-2 (ChR2)[11], *Volvox carteri* channelrhodopsin (VChR1)[12] and halorhodopsin[13,14]) to optically activate and inhibit neurons in nematodes[14–16]. Despite these remarkable developments, understanding the neuronal connections in *C. elegans* is still a daunting task: every connection has to be studied one at a time. An *in vivo* all-optical interrogation of the neural circuit that allows for simultaneous activation or inhibition of one or multiple neurons using channelrhodopsin or halorhodopsin and for simultaneous measurement of calcium activity in several other neurons would help surmount this limitation.

Two obstacles have to be overcome to achieve all-optical interrogation of neural circuits in this context. The first is that the excitation spectra of both channelrhodopsins (ChR2 and VChR1) and the genetically encoded calcium sensors (G-CaMP and Cameleon) overlap (**Fig. 1a**). When the fluorescent signal from the calcium sensors is measured, channelrhodopsins will be spuriously activated. The second challenge is to activate only one of several neurons expressing channelrhodopsins. Most neuronal promoters drive expression in multiple neurons. Thus, exposure of the worm to the excitation light will activate all neurons expressing ChR2 or VChR1. Moreover, to efficiently assay multiple connections, specific excitation of a select subset of neurons in worms expressing ChR2 or VChR1 in multiple neurons would be ideal.

We overcame both of these challenges to optically interrogate functional relations between neurons by using ChR2 and G-CaMP simultaneously. Our strategy allowed synchronous activation and recording from multiple neurons in intact worms to determine whether the functional connection from one neuron to another through both direct and indirect synapses is excitatory. As a proof of principle, we measured the functional properties of the connections from the sensory neuron ASH to the interneurons AVA and AVD as well as the connections between the interneurons RIM and AVA (**Fig. 1b**).

The *C. elegans* polymodal sensory neurons ASH detect noxious osmotic, mechanical and chemical stimuli; these stimuli induce calcium concentration increases in ASH neurons within seconds[17]. Proteins required for ASH cilia morphology, signal transduction and neurotransmission have been identified

[1]Faculty of Arts and Sciences Center for Systems Biology, [2]Department of Molecular and Cellular Biology and [3]School of Engineering and Applied Sciences, Harvard University, Cambridge, Massachusetts, USA. [4]Center for Cancer Research, Massachusetts General Hospital and Department of Pathology, Harvard Medical School, Charlestown, Massachusetts, USA. Correspondence should be addressed to S.R. (sharad@post.harvard.edu).

RECEIVED 26 JUNE; ACCEPTED 8 OCTOBER; PUBLISHED ONLINE 8 NOVEMBER 2009; DOI:10.1038/NMETH.1397

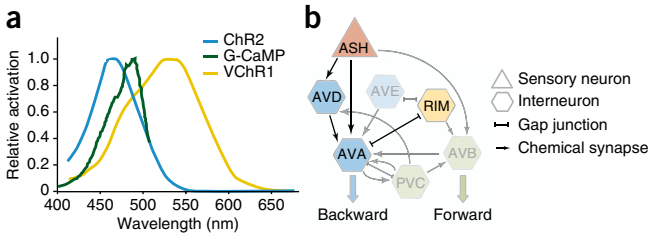

Figure 1 | Challenges facing an all-optical interrogation of neural circuits. (**a**) Excitation spectra of light-gated cation channels ChR2 and VChR1 (ref. 12) and of genetically encoded calcium sensor G-CaMP in the presence of 1 mM Ca^{2+} (ref. 7). (**b**) Schematic diagram showing the ASH neuron–mediated avoidance circuit: polymodal sensory neuron ASH detects repulsive stimuli; command interneurons AVA, AVD and AVE are critical for backward movement, AVB and PVC are critical for forward movement. RIM is an inter- or motorneuron with gap junctions to AVA and AVE. Direct chemical synapses and gap junctions based on electron microscopy reconstruction[2] between these neurons are also shown.

in previous genetic screens. OSM-3 kinesin is required for construction of the ASH sensory cilia distal segment. The OSM-9 TRP-family protein is required for robust response to osmotic, mechanical and chemical stimuli. The EAT-4 vesicular glutamate transporter[18] is required for stimulus-evoked release of the neurotransmitter glutamate[19]. The loss of genes encoding these proteins prevents behavioral response to most aversive chemical and mechanical stimuli. The critical synaptic targets of the ASH neurons have also been identified[2]; ASH neurons synapse directly and through other neurons onto the backward (AVA and AVD) and forward (AVB) command interneurons[3] (**Fig. 1b** and **Supplementary Fig. 1**).

RIM neurons may be multifunctional as they innervate muscles in the head region and synapse onto the backward and forward command interneurons, AVA, AVE and AVB[2] (**Fig. 1b**). It has previously been shown that when worms lacking RIM neurons had been removed from a food source, they showed a dramatic increase in the number of spontaneous reversals or, equivalently, a decrease in forward locomotion duration[20,21]. These results suggest that RIM neurons might have a role in regulating the frequency at which worms initiate backward movement.

We examined behavioral responses of *C. elegans* upon activating either ASH or RIM neurons using ChR2. Using our setup, we optically interrogated the functional connectivity of these neurons with the command interneurons, AVA and AVD.

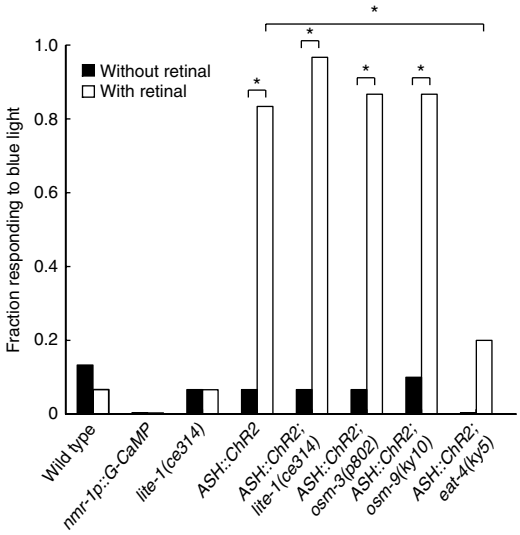

Figure 2 | Activation of ChR2 in ASH neurons by whole-body illumination. The fraction of worms of the indicated strains showing rapid reversal upon whole-body blue-light illumination is plotted. Thirty worms were tested for each strain, in the presence or absence of retinal. *ASH::ChR2* represents *sra-6p::ChR2*. *$P < 0.001$.

RESULTS

ChR2 activation of ASH neurons: behavioral response

We tested whether activating ASH sensory neurons using ChR2 evokes a behavioral avoidance response. We used the *sra-6* promoter to drive ChR2 expression in ASH neurons (*sra-6p::ChR2*)[22]. In the presence of retinal, a ChR2 cofactor, worms expressing the *sra-6p::ChR2* transgene exhibited an acute response to blue light (**Fig. 2** and **Supplementary Movie 1**). This light response was similar to the ASH neuron avoidance response to osmotic shock: both behaviors start with a rapid reversal and are followed by an omega turn. In the absence of retinal, worms expressing *sra-6p::ChR2* did not show an acute response to blue light (**Fig. 2**). These results indicate that directly depolarizing ASH neurons using ChR2 evoked a behavior similar to the native avoidance behavior. Our findings are consistent with previous studies using ChR2 (ref. 23) and heterologous expression of the mammalian TRPV1 channel in ASH neurons[24].

The blue light response of *sra-6p::ChR2* worms might be complicated by *C. elegans* avoidance of short-wavelength light (that is, blue to ultraviolet)[25,26]. Worms respond to blue-light illumination of the whole body with accelerated forward locomotion; *lite-1* gene function is required for this native light response[26]. The withdrawal response upon whole-body blue-light illumination in *sra-6p::ChR2* transgenic worms might be partially suppressed by the forward locomotion induced by the native light response. To address this, we examined *lite-1; sra-6p::ChR2* worms. In the presence of retinal, *lite-1; sra-6p::ChR2* worms initiated a more robust withdrawal response than *sra-6p::ChR2* worms (**Fig. 2**; $P < 0.05$). This is consistent with previous studies and suggests that loss of *lite-1* increases the propensity of worms to initiate reversals upon ChR2 excitation in ASH neurons.

We tested whether the avoidance response generated by ChR2 activation in ASH neurons depends on normal sensory signal transduction pathways and on ASH neurotransmission. The response in *osm-3* or *osm-9* worms was as robust as in wild-type ones, showing that direct activation of ASH neurons through exogenously expressed ChR2 is independent of the normal sensory apparatus. However, the ChR2-evoked avoidance response was greatly reduced in *eat-4* worms (**Fig. 2** and **Supplementary Movie 2**). This is consistent with previous studies demonstrating that loss of *eat-4* suppresses chemical, osmotic and nose-touch avoidance[19]. Thus, the behavioral response is neurotransmission-dependent and ChR2-evoked ASH neuron activation probably caused the release of glutamate as a primary neurotransmitter from these neurons.

ASH neurons synapse onto AVA and AVD interneurons. Classical cell ablation studies, in addition to genetic, electrophysiological and optical imaging studies, suggest that AVA and AVD regulate the switch from forward to backward locomotion. For example, spontaneous activity in AVA interneurons correlates with the initiation of reversals[9] (**Supplementary Fig. 2**). Thus the

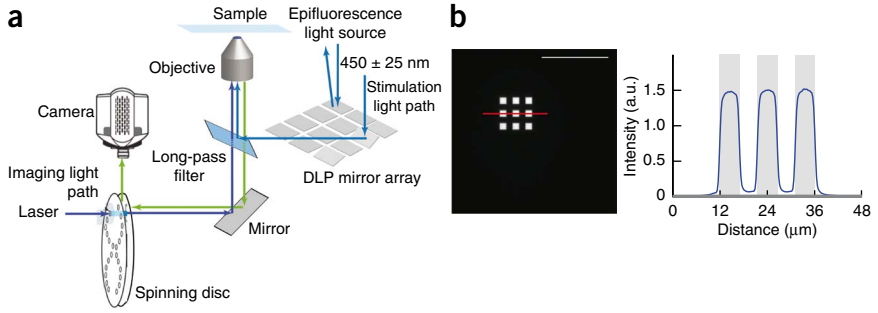

Figure 3 | Optical setup for ChR2 stimulation and simultaneous G-CaMP imaging. (**a**) The stimulation and imaging light paths are shown. In the stimulation light path, a high-power epifluorescence light source, used to excite ChR2, hits a digital light processing (DLP) mirror array before entering the objective. Each mirror in the DLP mirror array can be controlled independently. The number of mirrors turned on and their positions in the array determine the location and size of the spots on the sample. In the imaging light path, a low-power 488-nm laser coupled to a spinning disc and an electron-multiplying charge-coupled device camera was used to measure G-CaMP fluorescence. The light paths were independently controlled. (**b**) An image with nine 5 μm × 5 μm rectangular regions, each 5 μm apart from the other, illuminated using the DLP mirror array is shown (left). The intensity profile along the red line in the image (right, shaded regions indicate illuminated regions), showing sharp intensity differences between illuminated and dark regions, displaying the ability of the DLP mirrors to illuminate specific regions. Scale bar, 50 μm.

We measured G-CaMP fluorescence in worms expressing both G-CaMP and ChR2 in ASH neurons (*sra-6p::ChR2*; *osm-10p::G-CaMP*) using the 488-nm laser. ChR2 in ASH neurons was not substantially activated during this measurement, as indicated by the flat G-CaMP traces (**Figs. 4**, **5** and **Supplementary Figs. 3–11**). At the power level we used for G-CaMP measurements, worms rarely responded to illumination with avoidance behavior (data not shown). Upon reducing the laser power by a factor of 10 (power density, 0.01 mW mm^{-2}), we could still measure signals that were 3 s.d. above background (**Supplementary Fig. 3**). These results show that we can use low-intensity laser light for imaging G-CaMP fluorescence without substantially activating ChR2.

simplest model of the ASH neuron–mediated avoidance response is that the ASH sensory neurons activate the AVA interneurons as part of a functional avoidance circuit. We tested this hypothesis with the all-optical technique we developed.

Measuring G-CaMP signals

To selectively monitor calcium activity using G-CaMP in ChR2-expressing worms, we exploited the fact that ChR2 activation requires a combination of high intensity and/or a long duration of stimulation[27]. We used two different light paths and light sources, with the low-power 488-nm laser and a spinning disc to measure G-CaMP activity and a higher-power epifluorescence source to excite ChR2 (**Fig. 3**). The total power of 488-nm laser light measured at the back aperture of a ×63 objective was 10 μW. When combined with a 100 ms exposure time and 550 ms time interval between acquisitions, we estimated the power density at the back aperture of the ×63 objective to be 0.1 mW mm^{-2}.

Activating neurons expressing ChR2

We used a high-power blue light source to activate ChR2-expressing neurons. At the back aperture of the same ×63 objective, the power measured from this light source was 1,500 μW (power density 8 mW mm^{-2}; Online Methods), which ensures sufficient depolarization of ChR2-expressing neurons. To achieve specific excitation of a selected subset of neurons in worms expressing ChR2 in multiple neurons, we introduced a digital light processing (DLP) mirror array (**Fig. 3a**). By turning only one mirror in the

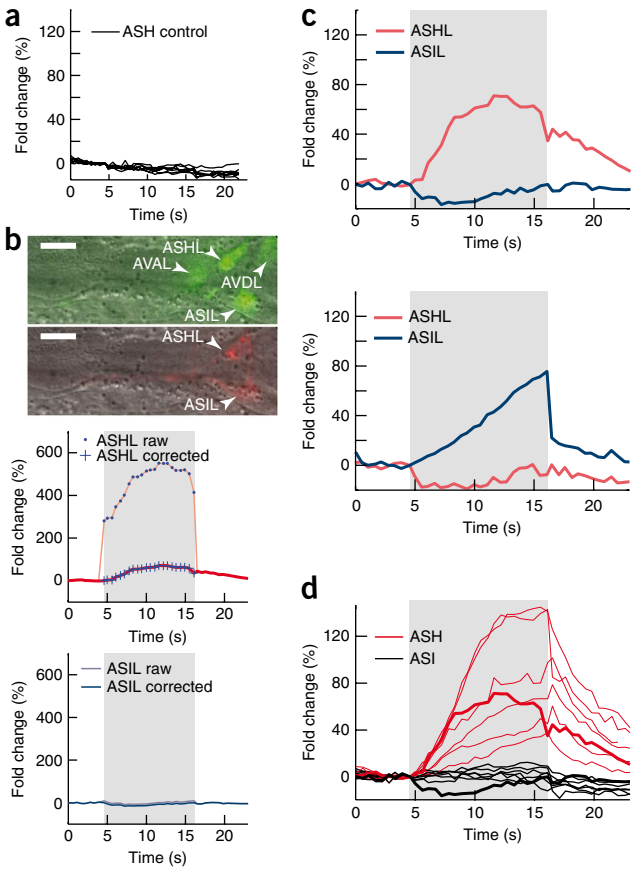

Figure 4 | Validation of specific stimulation *in vivo*. (**a**) G-CaMP fluorescence traces (6 traces in 6 worms) upon low-power laser illumination in worms that express both G-CaMP and ChR2 in ASH neurons. Fold change is the relative fluorescence increase over the fluorescence intensity before stimulation. (**b**) The left ASH (ASHL) and ASI (ASIL) neurons from which traces were recorded are shown. Green (G-CaMP) and red (ChR2-mCherry) fluorescence images superposed on differential interference contrast (DIC) images show these neurons as well as the left AVA (AVAL) and AVD (AVDL) neurons. Raw and corrected fold changes in G-CaMP fluorescence traces of ASHL (middle) and ASIL (bottom) neurons are shown during ASHL neuron stimulation using the DLP mirror array. Blue light used for ChR2 stimulation also excited G-CaMP in ASHL to produce an intensity jump. The jump was removed to give a corrected trace. The gray region indicates the time period during which ASHL was illuminated with the stimulation light. Scale bar, 10 μm. (**c**) Corrected G-CaMP fluorescence traces of ASHL and ASIL in **b**, plotted together for comparison (ASHL stimulation; top). Fluorescence traces of ASHL and ASIL neurons during ASIL stimulation in the same worm as in **b** (bottom). (**d**) Compiled traces for either left or right ASH and ASI neurons during ASH stimulation in 7 worms. The traces from the worm shown in **b** are plotted in thick lines.

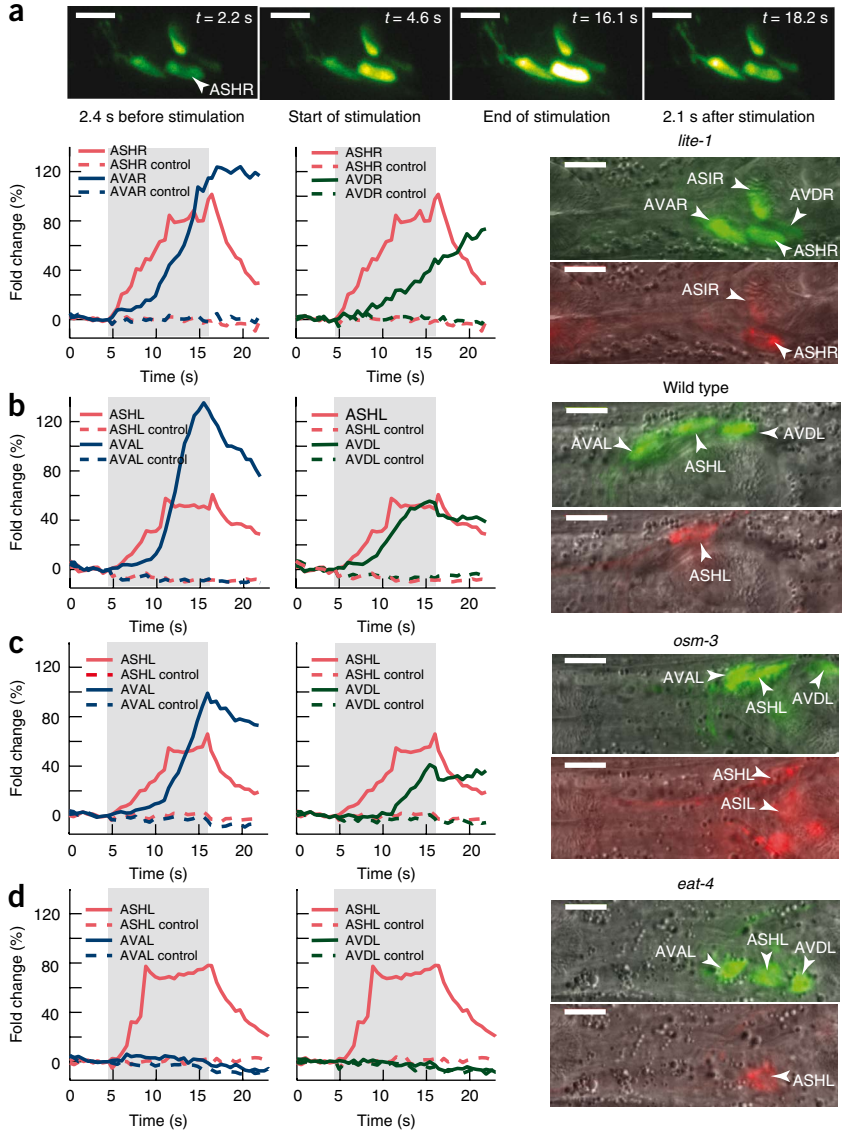

Figure 5 | Stimulation of ChR2 in ASH neuron activates AVA and AVD neurons. (**a**) Representative G-CaMP traces in ASH, AVA and AVD neurons in *lite-1(ce314)* during either left or right ASH (ASHL or ASHR) neuron stimulation (bottom left). Stills from the same time-lapse experiment are shown to illustrate fluorescence intensity changes in neurons, AVA and AVD, from the same side of the body (top). The gray region indicates the time period during which ASH neuron was stimulated. Control traces were obtained with the stimulation light turned off. The green and red fluorescence images superposed on DIC images (right; as in **Fig. 4**) are shown for the worm from which the traces were recorded. (**b**–**d**) Similar recordings for wild-type (**b**), *osm-3(p802)* (**c**) and *eat-4(ky5)* (**d**) backgrounds. Scale bar, 10 µm.

array to reflect light into the objective, a near diffraction-limited spot could be obtained on the target (~0.5 µm in diameter) at the focal plane of the objective. Therefore, by appropriate manipulation of mirrors, the sample could be illuminated with an arbitrary spatial pattern of light (**Fig. 3b**). As the objective lens has a high numerical aperture (NA) of 1.4, excitation of ChR2 can be restricted to a region near the focal plane where the power density of the focused light is the highest.

We tested the spatial resolution of the DLP mirror illumination *in vivo*. The *sra-6* promoter drives ChR2 expression in ASH and the nearby ASI sensory neurons. Using the DLP mirror system, we could specifically activate either ASH or ASI neurons in intact worms. The stimulation was specific, as we observed a large increase in G-CaMP fluorescence only in the excited neuron (**Fig. 4b–d**). In particular, multiple traces obtained from different worms showed that ASH neurons can be specifically excited while not exciting ASI in the same worm (**Fig. 4d**). In **Figures 5** and **6**, we displayed single traces corresponding to the shown fluorescence image of the worm, for clarity. Multiple traces as well as averages and s.e.m. are shown in **Supplementary Figures 8–15**, where appropriate.

Thus, by combining two light sources of different intensity, G-CaMP fluorescence can be measured without activating ChR2-expressing neurons. By using a DLP mirror array, specific neurons in a field of ChR2-expressing neurons can be activated. We used these tools to study two well-described *C. elegans* circuits: between ASH, AVA and AVD as well as between RIM and AVA neurons (**Fig. 1b**).

ASH sensory neurons activate AVA and AVD interneurons

To monitor the activities in AVA and AVD neurons upon ASH neuron stimulation, we used the *nmr-1* promoter to drive expression of G-CaMP in AVA, AVD, AVE, RIM and AVG interneurons[28]. Focused blue-light illumination of ASH neurons increased the intensity of G-CaMP fluorescence in ASH neurons (**Fig. 5a** and **Supplementary Movie 3**, **Supplementary Fig. 5a**, 59 ± 21% fluorescence fold increase compared with 0.5 ± 1% in control traces without light stimulation, $n = 9$, $P < 0.001$). After optical activation of ASH neurons, the G-CaMP fluorescence intensity in AVA and AVD neurons also increased, indicating that the activation of ASH neurons activated AVA and AVD neurons (**Fig. 5a** and **Supplementary Figs. 4**, **5a**, **6b**, 86 ± 38% fluorescence fold increase compared with 4 ± 8% in control traces for AVA neurons, $n = 8$, $P < 0.001$; 69 ± 34% fluorescence fold increase compared with 2 ± 2% in control traces for AVD neurons, $n = 5$, $P = 0.01$). The resulting change in G-CaMP fluorescence in AVA was comparable to that during spontaneous activity (**Supplementary Fig. 2**; $P = 0.4$), suggesting that ChR2 activation of ASH neurons resulted in physiological levels of activation in AVA neurons. For worms grown without retinal, illumination of ASH neurons did not activate either ASH or AVA neurons (**Supplementary Fig. 7**), indicating that the calcium activity seen in AVA neurons during ASH neurons stimulation was not due to spontaneous activity.

The activation from ASH to AVA and AVD neurons was similar in *lite-1*, wild-type and *osm-3* backgrounds (**Fig. 5b**,**c**, **Supplementary Figs. 5a–c**, **6a**,**b**, **8–10**). This suggests that *lite-1* did not affect the activation in ASH or AVA neurons and that optical excitation bypassed the sensory apparatus of ASH, consistent with behavioral analysis (**Fig. 2**).

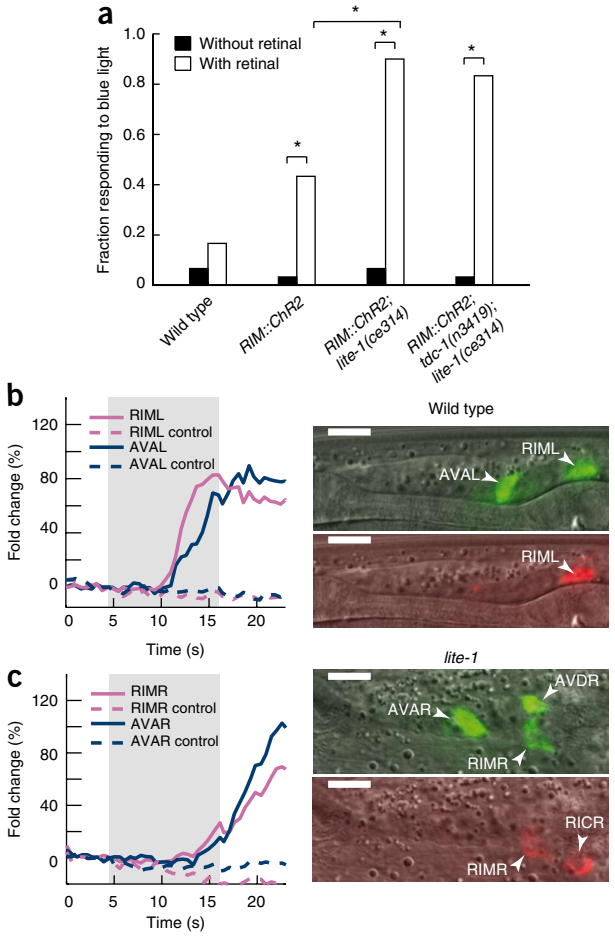

Figure 6 | Specific stimulation of ChR2 in RIM activates AVA and generates an avoidance response. (**a**) The fraction of worms that withdrew in response to blue light in the indicated strains. Thirty worms were tested in each genetic background in the presence or absence of retinal. *RIM::ChR2* represents *tdc-1p::ChR2*. *$P < 0.001$. (**b**,**c**) Representative G-CaMP traces in RIM and AVA neurons from the same side of the body (left or right) in the wild-type (**b**) and *lite-1(ce314)* (**c**) background (left). The gray region indicates the time period during which either the left or right RIM (L or R) neuron was activated with the stimulation light. Control traces were obtained with the stimulation light turned off. The green and red fluorescence images superposed on DIC (right, as in **Fig. 4**) are shown for the worms from which the traces were recorded. Scale bar, 10 µm.

We note that the calcium response in AVA after ASH stimulation is detected with a longer delay than the behavioral response after whole body illumination. Moreover, whether the activation of AVA and AVD neurons occurs via direct or indirect synaptic connections cannot be distinguished from these imaging experiments alone. We studied functional connections in mutant worms in which the ASH neuron–mediated avoidance behavior was affected. In worms lacking *eat-4* and thus deficient in glutamatergic vesicle loading, the activation of AVA and AVD by ASH neurons was greatly suppressed compared with worms in wild-type and *lite-1* backgrounds (**Fig. 5d**, **Supplementary Movie 4**, **Supplementary Figs. 5d**, **6c**, **11** and **Supplementary Note**, *eat-4* worms show $27 \pm 45\%$ fluorescence fold increase in AVA neurons, $n = 16$, $P = 0.004$ compared to wild type; 9 ± 5 % fluorescence fold increase in AVD neurons, $n = 6$, $P \leq 0.001$ compared to wild type). These results show that the functional connections from ASH neurons to both AVA and AVD neurons are predominantly glutamatergic and excitatory, consistent with our behavioral analysis (**Fig. 2**).

ChR2 activation of RIM interneurons: behavioral response

We examined another *C. elegans* circuit in which RIM interneurons are connected directly by gap junctions to AVA and AVE command interneurons[2] (**Fig. 1b**). We first determined that optical stimulation of RIM neurons using ChR2 increased the reversal frequency. We used the *tdc-1* promoter to drive expression of ChR2 in RIM (and faint or inconsistent expression in RIC)[21]. In the presence of retinal, worms expressing the *tdc-1p::ChR2* transgene responded to broad blue-light illumination by initiating a rapid withdrawal response followed by an omega turn, like the ASH neuron avoidance response (**Fig. 6a** and **Supplementary Movie 5**). In the absence of retinal, the worms did not respond to blue light, confirming that the withdrawal response was due to ChR2 activation. In the presence of retinal, worms expressing *tdc-1p::ChR2* in a *lite-1* background showed a more robust response than worms expressing the same transgene in a wild-type background as *lite-1* eliminated the native forward acceleration response to broad blue-light illumination (**Fig. 6a**).

tdc-1 encodes a tyrosine decarboxylase, which is required for the synthesis of tyramine[21]. Tyramine signaling inhibits egg laying, modulates reversal behavior and suppresses head oscillations in response to anterior touch. The light response in worms expressing ChR2 in RIM in the *tdc-1, lite-1* background was not significantly different from worms in *lite-1* background (**Fig. 6a**). This suggests that light activation of RIM neurons can modulate locomotion via a tyramine-independent mechanism; one possibility is that this occurs through signaling from RIM neurons through direct gap junctions to the backward command interneurons AVA and AVE. To test this, we studied mutants in *unc-9*, which encodes an innexin, a major component of *C. elegans* gap junctions[29], bearing in mind that *unc-9* might broadly affect the nervous system. The light response in worms expressing ChR2 in RIM neurons in *lite-1, unc-9* background was significantly reduced compared with worms expressing ChR2 in RIM in *lite-1* background (**Supplementary Fig. 12;** $P < 0.001$). This decrease in response is not because those worms cannot move backward: both anterior body touch and ChR2 activation in ASH neurons in *lite-1, unc-9* worms evoked robust reversals (**Supplementary Fig. 12**). Thus, the activation of AVA neurons owing to acute RIM neuron activation might occur predominantly through gap junctions, with the caveat that *unc-9* worms could have other defects besides dysfunctional gap junctions.

RIM neurons activate AVA interneurons

Spatially focused blue-light illumination of RIM neurons in *tdc-1p::ChR2; nmr-1p::G-CaMP* worms increased the intensity of G-CaMP fluorescence in RIM neurons, suggesting that ChR2 in RIM neurons raises calcium levels and activates RIM neurons (**Fig. 6b**,**c**, **Supplementary Movie 6** and **Supplementary Figs. 13–15**, $95 \pm 31\%$ fluorescence fold increase compared with $2 \pm 2\%$ in control traces in wild type background, $n = 8$, $P < 0.001$; $70 \pm 36\%$ fluorescence fold increase compared with $4 \pm 11\%$ in control traces in *lite-1* background, $n = 5$, $P = 0.017$). After the activation of RIM, the G-CaMP fluorescence intensity in AVA interneurons also increased, indicating that the activation of RIM neurons activated AVA interneurons (**Fig. 6b**,**c** and **Supplementary Figs. 13–15**, $90 \pm 43\%$ fluorescence fold increase compared with $1 \pm 2\%$ in control traces in the wild-type background, $n = 8$, $P < 0.001$; $87 \pm 32\%$ fluorescence fold increase compared with $1 \pm 1\%$ in control traces in *lite-1*

background, $n = 5$, $P = 0.004$). RIM neurons have multiple gap junctions with AVA neurons and also have indirect connections to AVA neurons through AVE and AVB neurons[2] (**Fig. 1b** and **Supplementary Fig. 1**). Our results, in conjunction with the behavioral analysis (**Supplementary Fig. 12**) suggest that activation of AVA neurons owing to RIM neuron activation may occur through gap junctions.

DISCUSSION

Using low light levels to measure calcium activity, we avoided activating neurons expressing ChR2. G-CaMP is much dimmer than native fluorescent proteins[30]. With the newly developed calcium indicators G-CaMP1.6 (~40 times brighter than G-CaMP) and G-CaMP2 (~200 times brighter than G-CaMP)[30], the strategy of using low light intensity for G-CaMP imaging to avoid ChR2 activation might well be applied to other neuronal circuits in *C. elegans* or even other organisms. By quickly changing the wavelength filter in the excitation light path, the ability to incorporate and simultaneously excite halorhodopsin in other neurons is a relatively easy extension. By coordinating a piezo *Z*-drive with the optical setup, neurons in different focal planes can also be stimulated and monitored (**Supplementary Fig. 16**).

The all-optical technique we described can be used to map functional relations between neurons, but the method cannot be used at present to dissect direct versus indirect synaptic connections. Typically, it took a few seconds to detect a substantial fluorescence rise in AVA neuron after ASH neuron was stimulated (**Supplementary Note**). In contrast, worms typically responded to whole-body blue-light illumination by initiating backward movement within 1 s in the behavior assay (data not shown). The limited sensitivity and slow kinetics of G-CaMP[30] might contribute to this discrepancy besides many other factors (**Supplementary Note**) and thus may preclude the ability to ascribe the functional connections measured here to specific direct or indirect synaptic connections.

When combined with the physical connectivity data[2], the all-optical method can be used to infer relative contributions of synaptic connections by studying functional connections in mutant worms in which specific synaptic connections have been disrupted. Such measurements can help focus our attention on specific neurons and synapses for careful electrophysiological interrogation. With the improvement of genetically encoded calcium indicators or using faster voltage-sensitive indicators, the all-optical method we proposed here will provide more details about functional and synaptic connections.

METHODS

Methods and any associated references are available in the online version of the paper at http://www.nature.com/naturemethods/.

Note: Supplementary information is available on the Nature Methods website.

ACKNOWLEDGMENTS

We thank P. Swain and S. H. Simon for discussions, members of the *Caenorhabditis* Genetic Center (CGC) for strains, J. Naki (RIKEN Brain Science Institute) for G-CaMP plasmid, A. Gottschalk (Goethe University Frankfurt) for *chop-2(H134R)* cDNA and A. Fire (Stanford University) for plasmid vectors. Z.V.G. thanks A. Ahmed, M. Debono and A. Desai for 2007 *C. elegans* course. A.C.H. was supported by the US National Institute of General Medical Sciences.

AUTHOR CONTRIBUTIONS

Z.V.G., A.C.H. and S.R. planned different aspects of the work. Z.V.G. performed all the experiments. Z.V.G. and S.R. wrote the manuscript.

Published online at http://www.nature.com/naturemethods/.
Reprints and permissions information is available online at http://npg.nature.com/reprintsandpermissions/.

1. Brenner, S. The genetics of *Caenorhabditis elegans*. *Genetics* **77**, 71–94 (1974).
2. White, J.G., Southgate, E., Thomson, J.N. & Brenner, S. The structure of the nervous system of the nematode *Caenorhabditis elegans*. *Phil. Trans. R. Soc. Lond. B* **314**, 1–340 (1986).
3. Chalfie, M. *et al.* The neural circuit for touch sensitivity in *Caenorhabditis elegans*. *J. Neurosci.* **5**, 956–964 (1985).
4. Bargmann, C.I. & Avery, L. Laser killing of cells in *Caenorhabditis elegans*. *Methods Cell Biol.* **48**, 225–250 (1995).
5. de Bono, M. & Maricq, A.V. Neuronal substrates of complex behaviors in *C. elegans*. *Annu. Rev. Neurosci.* **28**, 451–501 (2005).
6. Goodman, M.B., Hall, D.H., Avery, L. & Lockery, S.R. Active currents regulate sensitivity and dynamic range in *C. elegans* neurons. *Neuron* **20**, 763–772 (1998).
7. Nakai, J., Ohkura, M. & Imoto, K. A high signal-to-noise Ca(2+) probe composed of a single green fluorescent protein. *Nat. Biotechnol.* **19**, 137–141 (2001).
8. Miyawaki, A. *et al.* Fluorescent indicators for Ca2+ based on green fluorescent proteins and calmodulin. *Nature* **388**, 882–887 (1997).
9. Chronis, N., Zimmer, M. & Bargmann, C.I. Microfluidics for *in vivo* imaging of neuronal and behavioral activity in *Caenorhabditis elegans*. *Nat. Methods* **4**, 727–731 (2007).
10. Kerr, R. *et al.* Optical imaging of calcium transients in neurons and pharyngeal muscle of *C. elegans*. *Neuron* **26**, 583–594 (2000).
11. Nagel, G. *et al.* Channelrhodopsin-2, a directly light-gated cation-selective membrane channel. *Proc. Natl. Acad. Sci. USA* **100**, 13940–13945 (2003).
12. Zhang, F. *et al.* Red-shifted optogenetic excitation: a tool for fast neural control derived from *Volvox carteri*. *Nat. Neurosci.* **11**, 631–633 (2008).
13. Han, X. & Boyden, E.S. Multiple-color optical activation, silencing, and desynchronization of neural activity, with single-spike temporal resolution. *PLoS One* **2**, e299 (2007).
14. Zhang, F. *et al.* Multimodal fast optical interrogation of neural circuitry. *Nature* **446**, 633–639 (2007).
15. Nagel, G. *et al.* Light activation of channelrhodopsin-2 in excitable cells of *Caenorhabditis elegans* triggers rapid behavioral responses. *Curr. Biol.* **15**, 2279–2284 (2005).
16. Liewald, J.F. *et al.* Optogenetic analysis of synaptic function. *Nat. Methods* **5**, 895–902 (2008).
17. Hilliard, M.A. *et al.* *In vivo* imaging of *C. elegans* ASH neurons: cellular response and adaptation to chemical repellents. *EMBO J.* **24**, 63–72 (2005).
18. Lee, R.Y., Sawin, E.R., Chalfie, M., Horvitz, H.R. & Avery, L. EAT-4, a homolog of a mammalian sodium-dependent inorganic phosphate cotransporter, is necessary for glutamatergic neurotransmission in *Caenorhabditis elegans*. *J. Neurosci.* **19**, 159–167 (1999).
19. Berger, A.J., Hart, A.C. & Kaplan, J.M. G alphas-induced neurodegeneration in *Caenorhabditis elegans*. *J. Neurosci.* **18**, 2871–2880 (1998).
20. Gray, J.M., Hill, J.J. & Bargmann, C.I. A circuit for navigation in *Caenorhabditis elegans*. *Proc. Natl. Acad. Sci. USA* **102**, 3184–3191 (2005).
21. Alkema, M.J., Hunter-Ensor, M., Ringstad, N. & Horvitz, H.R. Tyramine Functions independently of octopamine in the *Caenorhabditis elegans* nervous system. *Neuron* **46**, 247–260 (2005).
22. Troemel, E.R., Chou, J.H., Dwyer, N.D., Colbert, H.A. & Bargmann, C.I. Divergent seven transmembrane receptors are candidate chemosensory receptors in *C. elegans*. *Cell* **83**, 207–218 (1995).
23. Bacaj, T., Tevlin, M., Lu, Y. & Shaham, S. Glia are essential for sensory organ function in *C. elegans*. *Science* **322**, 744–747 (2008).
24. Tobin, D. *et al.* Combinatorial expression of TRPV channel proteins defines their sensory functions and subcellular localization in *C. elegans* neurons. *Neuron* **35**, 307–318 (2002).
25. Ward, A., Liu, J., Feng, Z. & Xu, X.Z. Light-sensitive neurons and channels mediate phototaxis in *C. elegans*. *Nat. Neurosci.* **11**, 916–922 (2008).
26. Edwards, S.L. *et al.* A novel molecular solution for ultraviolet light detection in *Caenorhabditis elegans*. *PLoS Biol.* **6**, e198 (2008).
27. Wang, H. *et al.* High-speed mapping of synaptic connectivity using photostimulation in Channelrhodopsin-2 transgenic mice. *Proc. Natl. Acad. Sci. USA* **104**, 8143–8148 (2007).
28. Brockie, P.J., Madsen, D.M., Zheng, Y., Mellem, J. & Maricq, A.V. Differential expression of glutamate receptor subunits in the nervous system of *Caenorhabditis elegans* and their regulation by the homeodomain protein UNC-42. *J. Neurosci.* **21**, 1510–1522 (2001).
29. Liu, Q., Chen, B., Gaier, E., Joshi, J. & Wang, Z.W. Low conductance gap junctions mediate specific electrical coupling in body-wall muscle cells of *Caenorhabditis elegans*. *J. Biol. Chem.* **281**, 7881–7889 (2006).
30. Kotlikoff, M.I. Genetically encoded Ca2+ indicators: using genetics and molecular design to understand complex physiology. *J. Physiol. (Lond.)* **578**, 55–67 (2007).

ONLINE METHODS

Strains. *C. elegans* strains were maintained under standard conditions[1], unless otherwise indicated. Wild-type worms were Bristol strain N2. Germline transformations were implemented as described[31]. Extrachromosomal array *sraEx47* was integrated into chromosomes using γ-ray irradiation. The resulting integrated strains were backcrossed to the N2 at least 8 times. Standard crosses were used to transfer the extrachromosomal arrays *sraEx80* and *sraEx83* into different genetic backgrounds. The success of genetic crosses was checked using the hydrophobic cyanine dye DiI staining of amphid neurons (*osm-3(p802)*), PCR (*tdc-1(n3419)*), blue-light avoidance assay (*lite-1(ce314)*), monitoring pharyngeal pumping rate (*eat-4(ky5)*) and osmotic drop assay (*eat-4(ky5), osm-3(p802)* and *osm-9(ky10)*). The genotypes used are listed as follows: N2 (wild type), *eat-4(ky5)*, *lite-1(ce314), osm-3(p802), osm-9(ky10)* and *tdc-1(n3419)*. Transgenic strains generated during this work are listed in **Supplementary Table 1**.

Molecular biology. *chop-2(H134R)::mCherry* was obtained by swapping mCherry with YFP in *chop-2(H134R)::YFP*[15]**.** We used a 5.1-kb *nmr-1* promoter that had been previously described[28]. We amplified 4-kb *sra-6*, 4.4-kb *tdc-1*, 0.8-kb *unc-122* and 2.9-kb *F55B11.3* promoters by PCR from *C. elegans* genomic DNA. All the promoters were cloned into the Fire lab vector kit plasmid pPD95.75 in which the sequence encoding GFP was replaced either by the sequence encoding G-CaMP or by *chop-2 (H134R)::mCherry*. The homozygous deletion of *tdc-1* was checked by PCR amplification. Primers used for PCR are listed in **Supplementary Table 2**.

Intensity measurement. A Newport 841-P USB power meter was used to measure the power of blue light reaching the Nematode Growth Medium (NGM) cultivation plate in each assay. The intensity of light reaching the culture plate for behavior assay was controlled using a combination of the click stop iris on the X-Cite Illuminator and the iris on the ZEISS Discovery dissecting microscope. The intensity used for behavioral assays (**Figs. 2**,**6** and **Supplementary Fig. 12**) was 10 mW mm^{-2}. To measure the intensity of the exciting blue light from lambda DG-4, a region was specified by DLP mirror array and the total power was used to calculate the intensity for stimulation. The intensity used for ChR2 stimulation was 8.0 mW mm^{-2}, which is comparable to the intensity used for behavioral assays (**Supplementary Fig. 17**). The intensity of the 488-nm laser used to monitor G-CaMP fluorescence was about 0.1 mW mm^{-2}, unless otherwise mentioned.

Behavioral assays. ChR2 requires the cofactor all-*trans*-retinal (ATR) for function. An overnight LB culture of *Escherichia coli* (strain OP50) was concentrated 20 times and mixed with ATR (Sigma) for a final concentration of 100 μM. We spread 300 μl of this bacteria-ATR suspension onto NGM plates. Mid-L4 larval worms expressing appropriate *mCherry* markers were selected the day before the experiment and cultivated on the newly seeded NGM plates overnight. A motorized ZEISS Discovery dissecting microscope equipped with a 120 W X-Cite lamp was used for all the avoidance behavior assays. An EGFP filter 480/40 nm was used to filter blue light for illumination. Young adult worms, slowly moving forward on the cultivation plate, were illuminated with blue light for about 1 s. Worms initiating backward movement during or within 1 s after illumination were scored as 1. Worms that accelerated forward movement, paused or initiated backward movement after 1 s of the end of illumination were scored as 0. The response of typically 30 worms was averaged to obtain the fraction of worms responding to blue light.

Statistical analyses. The standard chi-square test was used to determine the significance of the data for behavioral assays shown in **Figures 2**, **6** and **Supplementary Figure 12**. Welch's *t*-test was used to compare (i) the activation level in ASH and AVA in wild type, *lite-1, osm-3* and *eat-4* genetic background during ASH stimulation; (ii) the activation level in AVA during spontaneous reversals and during ASH or RIM stimulation; (iii) the activation delay in AVA in wild-type, *lite-1, osm-3* and *eat-4* genetic background (**Supplementary Note**). The amplitude of G-CaMP fluorescence fold change due to ASH or RIM neuron stimulation is defined as the maximum fold change after start of stimulation.

Optical stimulation and calcium imaging. Young adult worms were treated with 10-mM muscimol on a hydrated agar pad for imaging; muscimol, a GABA agonist, halts muscle contraction and worms developed a flaccid paralysis[32]. Immobilizing worms using muscimol was more convenient and typically gave more robust and reproducible optical signals compared to immobilizing worms using glue in our hands. For each stimulation experiment, a control experiment was performed with the activating light turned off, to show that there was no detectable G-CaMP fluorescence change during measurement. Then ChR2-expressing neurons were specifically stimulated while calcium activities in G-CaMP expressing neurons were monitored. Control measurements were also performed on worms grown without the ChR2 cofactor ATR.

Optical stimulations and recordings were performed on a Zeiss 200M inverted microscope. The microscope and all the other components were controlled by Metamorph software (version 7.5.3, Molecular Devices). Objective used was a ×63, NA = 1.4 Plan-Aprochromat oil objective. Neurons expressing *chop-2 (H134R)::mCherry* were identified using a Hamamatsu Orca-ER digital camera (C4742-80-12AG). Emission of mCherry was visualized at 650 nm (75-nm bandwidth) upon excitation at 565 nm (55-nm bandwidth). A high-speed Yokogawa CSU10 spinning disk confocal system equipped with DM488_BF488 filter set was used for imaging calcium activity and G-CaMP fluorescence was collected at 2 frames s^{-1} using a Hamamatsu electron-multiplying charge-coupled device (EM-CCD) digital camera (C9100-13). A digital-light-processing mirror array (Photonics Instrument) was used to generate a spatial mask that was subsequently used to deliver light for stimulation. A Lambda DG-4 optical switch equipped with a 300-W xenon lamp (Sutter Instrument) was used to deliver blue light, filtered with a HQ450/50X (Chroma) set, to activate ChR2. The power of the excitation light intensity from the DLP mirrors (8 mW mm^{-2}) was comparable to the excitation intensities where about 90% of the worms showed a behavioral response (**Supplementary Fig. 17**). A 475-nm long-pass filter was used to reflect blue light up to the objective for stimulation. For stimulating and imaging neurons on different focal planes, a NanoscanZ piezo stage system (Prior Scientific) was used to switch between different focal planes within 10 ms.

Calcium imaging data analysis. Images stacks (TIFF files) were analyzed by custom written scripts for Matlab (Mathworks). For each neuron, an approximate region of interest was defined by a rectangular region of 10 μm × 10 μm surrounding that neuron. The exact size of the region of interest was slightly adjusted to exclude the adjacent neurons. The fluorescence intensity within the region of interest F, as described[33], was calculated as the mean intensity of the brightest 128 pixels (~8 μm^2) minus the mean intensity of a background region that was far away from the body. The average fluorescence intensity within 2 s before stimulation was taken as the basal signal (F_0). The percentage change in fluorescence intensity for the region of interest relative to the initial intensity F_0, $(F - F_0)/F_0 \times 100\%$, was plotted as a function of time for all the activation experiments. Because the excitation spectra of ChR2 and G-CaMP overlap, blue light used for stimulating ChR2 neurons also excites G-CaMP, which produced a jump in G-CaMP fluorescence intensity (**Fig. 4b** and **Supplementary Fig. 18**). This immediate jump in fluorescence is directly proportional to the fold change in the illumination intensity of the neuron that is excited (since in the range of power intensities we operate, the signal from G-CaMP is proportional to the power of the excitation light). During the period of stimulation, the G-CaMP signal is amplified (compared to when there is no stimulation) by a constant factor that is equal to the fold change in the illumination intensity. To eliminate the effects of this jump we divide the G-CaMP fluorescent signal during the period of excitation by the magnitude of this initial jump. The photobleaching of G-CaMP over the duration of the light stimulation (10 s), due to the stimulating light, was 1.2 ± 0.8% ($n = 6$, tested on worms fed without retinal) and thus was not corrected. The photobleaching of G-CaMP during measurement was even smaller and within measurement noise. Different numbers of pixels, 256 and 64, were also chosen to calculate the percentage change of fluorescence intensity and the results were not different from using 128 pixels (**Supplementary Fig. 19**). Thus, 128 pixels were used unless otherwise specified. Schematic guides to **Supplementary Movies 3**, **4** and **6** are shown in **Supplementary Figure 20**.

31. Mello, C.C., Kramer, J.M., Stinchcomb, D. & Ambros, V. Efficient gene transfer in *C. elegans*: extrachromosomal maintenance and integration of transforming sequences. *EMBO J.* **10**, 3959–3970 (1991).
32. McIntire, S.L., Jorgensen, E. & Horvitz, H.R. Genes required for GABA function in *Caenorhabditis elegans*. *Nature* **364**, 334–337 (1993).
33. Clark, D.A., Gabel, C.V., Gabel, H. & Samuel, A.D. Temporal activity patterns in thermosensory neurons of freely moving *Caenorhabditis elegans* encode spatial thermal gradients. *J. Neurosci.* **27**, 6083–6090 (2007).

doi:10.1038/nmeth.1397